# Cost-efficient polyurea carrier for precise control of an anti-inflammatory drug loading and release

Gabriele A. Pedroza, Lucia H. G. M. C. Macedo, Ricardo de Oliveira Bordonal, Natalia N. Silveira, Renato P. Orenha, Renato L. T. Parreira, Raquel A. dos Santos, Yann Molard, Maria Amela-Cortes, Eduardo F. Molina

▶ **To cite this version:**

Gabriele A. Pedroza, Lucia H. G. M. C. Macedo, Ricardo de Oliveira Bordonal, Natalia N. Silveira, Renato P. Orenha, et al.. Cost-efficient polyurea carrier for precise control of an anti-inflammatory drug loading and release. Journal of Drug Delivery Science and Technology, 2022, 76, pp.103744. 10.1016/j.jddst.2022.103744 . hal-03798136

**HAL Id: hal-03798136**
**https://hal.science/hal-03798136**

Submitted on 16 Nov 2022

**HAL** is a multi-disciplinary open access archive for the deposit and dissemination of scientific research documents, whether they are published or not. The documents may come from teaching and research institutions in France or abroad, or from public or private research centers.

L'archive ouverte pluridisciplinaire **HAL**, est destinée au dépôt et à la diffusion de documents scientifiques de niveau recherche, publiés ou non, émanant des établissements d'enseignement et de recherche français ou étrangers, des laboratoires publics ou privés.

Distributed under a Creative Commons Attribution - NonCommercial 4.0 International License

Journal Pre-proof

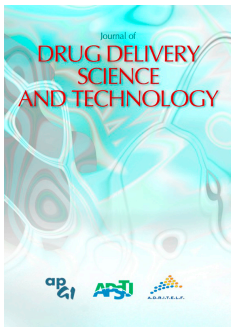


# Cost-efficient polyurea carrier for precise control of an anti-inflammatory drug loading and release

Gabriele A. Pedroza, Lucia H.G.M.C. Macedo, Ricardo de Oliveira, Natália S. Nascimento, Renato P. Orenha, Renato L.T. Parreira, Raquel Santos, Yann Molard, Maria Amela-Cortes, Eduardo F. Molina

PII: S1773-2247(22)00655-4

DOI: https://doi.org/10.1016/j.jddst.2022.103744

Reference: JDDST 103744

To appear in: *Journal of Drug Delivery Science and Technology*

Received Date: 2 May 2022

Revised Date: 17 August 2022

Accepted Date: 22 August 2022

Please cite this article as: G.A. Pedroza, L.H.G.M.C. Macedo, R. de Oliveira, Natá.S. Nascimento, R.P. Orenha, R.L.T. Parreira, R. Santos, Y. Molard, M. Amela-Cortes, E.F. Molina, Cost-efficient polyurea carrier for precise control of an anti-inflammatory drug loading and release, *Journal of Drug Delivery Science and Technology* (2022), doi: https://doi.org/10.1016/j.jddst.2022.103744.

This is a PDF file of an article that has undergone enhancements after acceptance, such as the addition of a cover page and metadata, and formatting for readability, but it is not yet the definitive version of record. This version will undergo additional copyediting, typesetting and review before it is published in its final form, but we are providing this version to give early visibility of the article. Please note that, during the production process, errors may be discovered which could affect the content, and all legal disclaimers that apply to the journal pertain.

© 2022 Published by Elsevier B.V.

Graphical abstract

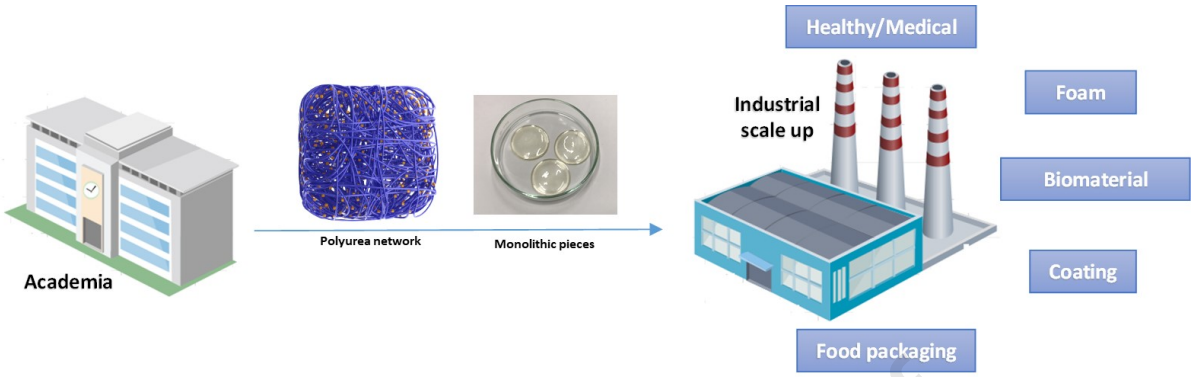


Journal Pre-proof

Journal Pre-proof

# Cost-efficient Polyurea Carrier for Precise Control of an anti-inflammatory Drug Loading and Release

*Gabriele A. Pedroza,[1] Lucia H. G. M. C. Macedo,[1] Ricardo de Oliveira,[1] Natália S. Nascimento,[1] Renato P. Orenha,[1] Renato L. T. Parreira,[1] Raquel Santos,[1] Yann Molard,[2] Maria Amela-Cortes,[2] Eduardo F. Molina*[*1]*

[1]*Universidade de Franca, Av. Dr. Armando Salles Oliveira 201, 14404-600 Franca, SP, Brazil*

[2]*Université Rennes, CNRS, ISCR - UMR 6226, ScanMAT – UMS 2001, F-35000 Rennes, France*

Corresponding author: Eduardo F. Molina
*email: eduardo.molina@unifran.edu.br
ORCID : 0000-0002-3574-2923

Journal Pre-proof

Journal Pre-proof


## Abstract

In this paper, we present a cost-efficient and reliable route to produce polyurea xerogel (PolyU) as a versatile carrier that provides a high drug loading and offers a tuning over diclofenac (DCF) release profile. A simple one-pot reaction of an amino-terminated-polyether-PEO and a crosslinker, hexamethylene diisocyanate trimer-HDI, allow us to obtain the polymeric networks. The gelation time during the sol-gel reactions (hydrolysis and condensation) can be modulated from minutes to hours by using acetone as solvent to achieve a decrease of reactivity between amine groups from PEO with isocyanate from HDI crosslinker. The interactions of PolyU networks and DCF drug was in depth evaluated by Fourier Transform Infrared Spectroscopy (FTIR), small angle X-ray scattering (SAXS) and computational studies. Analysis performed by differential scanning calorimetry (DSC) have confirmed the inhibition of crystalline moities of PEO by drug interactions with the PEO chains. PolyU was investigated in cell toxicity studies, showing no significant cytotoxicity against the CHO-K1 cell line. Considering the abundance of raw materials and cost-efficient for polyurea preparation, this work clearly opens up high prospects and provides a solution for scaling up the fabrication of new functional devices (contact lenses, patches, thin films, etc) with broad applications in the medical/health fields.


*Keywords: sol-gel, polyetheramine, isocyanate crosslink, microphases, small angle X-ray scattering.*

Journal Pre-proof

Journal Pre-proof

## 1. Introduction

Polymer derivated materials are usually applied as carrier for delivery and control release of drugs [1], proteins [2], therapeutic compounds [3], inorganic particles [4] showing advanced functions such as imaging agents for analytics and diagnostics [5], targeted delivery [6], controlled encapsulation [7], and more. However, the methodology used to produce these materials are often not economically viable and do not meet the requirements for production on an industrial scale. Therefore, many efforts have been made aiming to develop such carrier technologies by using, for example, electrospinning [8] or microfluidic [9] methods that allow a fine control over their monodispersity, structures, and compositions.

Polyurea is an elastomer polymer obtained from the reaction of polyamines and polyisocyanates resulting in the formation of urea linkages (-NH-CO-NH-) [10]. This class of polymer receives continuous attention from the scientific community, in particular, due to i) the absence of a catalyst during the reactions [11], ii) its high thermal/chemical stability [12,13], ii) its facile processability and iv) its resistance to UV radiation [14]. Polyurea elastic network shows microphase separation of two immiscible, covalently connected components, known as “hard” and “soft” domains. The “hard” domains act as physical cross-linker to reinforce the elastomer, while the “soft” domains form the continuous phase provide elasticity [15]. Furthermore, polyurea networks exploiting the hydrogen-bonding directionality (i.e. well-defined secondary structures) are of particular interest as supramolecular polymers [16-18].

Zhang et. al [12] produced new polyurea thin-film membranes for extreme pH nanofiltration. The fabricated membranes, based on branched polyethyleneimine, piperazine, and multi-isocyanate monomers, showed excellent acid/alkali resistance after exposure to HCl, $H_2SO_4$ and NaOH solutions (20 wt/v%) and are suitable for the treatment of industrial wastewater. By using commercially available reagents, Paraskevopoulou et al. [19] obtained polyurea-crosslinked calcium alginate beads (X-Ca-alg). The authors reported that X-Ca-alg biopolymers are robust materials compared to conventional Ca-alginate aerogels that are mechanically weak, and have

Journal Pre-proof

pratical applications including environmental remediation. In another work, polyurea was used as microcapsule to incorporate phexim pesticide for agriculture purposes. The phoxim-loaded polyurea showed high UV-resistance ability and can prolonge the effective duration of pesticide. It may be also applied as microcapsule for others pesticides [14].

Reports of polyurea as carrier for drug delivery systems are scarce [20-23]. In this work, we present a facile preparation of a polyurea xerogel with capacity to incorpotate high amounts (up to 30 wt%) of an anti-inflamatory drug. Diclofenac sodium (DCF) was chosen for this study. It has both analgesic and antipyretic properties and is classicaly used for the treatment of degenerative joint diseases such as rheumatoid arthritis, osteoarthritis. Administrated by ocular route, it is used in the management of ocular pathologies treated by surgery. Its low biological half-life (1 or 2 hours) implies multiple dosing to keep its therapeutic blood level, which often leads to adverse side effects in a long-term administration such as gastrointestinal bleeding, disturbances or peptic ulceration. Therefore, its controled release should provide extended therapeutic benefits with minimal local irritation.

The polyurea obtained in this work is a low-cost material that contains flexible polyetheramine blocks connected to an isocyanate trimer to form urea linkages. It is produced by a facile one-pot sol-gel reaction, which is a scalable, powerful and economically viable method, offering fine control over structure and loaded amount of drugs. The objectives of this work are to investigate in depth the i) visual polyurea gelation time as a function of monomers contact time with a solvent, ii) the biocompatibility of the matrix through citotoxicity studies, iii) the influence of the drug content on the structure of polyurea, iv) the release profile and kinetic mechanisms as a function of drug load. In particular, we show that the diclofenac drug release profile can be modulated by the interactions between DFC drug and the polyurea matrix as well as by the loaded drug amount.

Journal Pre-proof

## 2. Experimetal and characterizations

*2.1 Materials*: Diclofenac sodium salt DCF ($C_{14}H_{10}Cl_2NNaO_2$) and acetone (ACS reagent, ≥99.5%) were purchased from Sigma-Aldrich. O,O'-bis-(2-aminopropyl)polypropylene glycol-block-polyethylene glycol-block-polypropylene (Jeffamine ED2003 - PEO block with a molecular weight of 1900 g $mol^{-1}$) and the hexamethylene diisocyanate trimer-HDI (Desmodur N3300 with a molecular weight of ~ 504 g $mol^{-1}$) were donated by Huntsman Performance Products (Brazil) and Bayer Corporation, respectively. The Jeffamine ED2003 and Desmodur N3300 are reagents commercially avaliable from Huntsman and Bayer. All reagents were used without further purification.

*2.2 Synthesis of polyurea gels*: The polyurea xerogel was obtained by organic polycondensation reaction (sol-gel process) as reported in literature [24-26]. In brief, tridentate ligand HDI was covalently bonded to the PEO (Jeffamine ED-2003) by reaction of the isocyanate groups of HDI and the primary amino groups attached to the end of the polyether backbone of PEO (**Scheme 1**). In brief, 4 g of PEO macromer (2.10 x $10^{-3}$ mol) and 1 g of HDI cross-linker (1.98 x $10^{-3}$ mol) were completely dissolved using acetone in two separated beakers. These were sealed and stirred for 2h, at room temperature (~25°C), to form a homogenous solutions. The HDI solution was added dropwise to the PEO solution, while stirring at room temperature, until complete dissolution. The resulting solution was poured into Teflon® mold and kept at 25°C for 24 h for gelation.

*2.3 Synthesis of polyurea gels containing diclofenac drug*: Polyurea samples containing DCF were prepared *via* one-step sol-gel process. The desired drug amount (from 1 to 30 wt% with respect to the mass of PEO) was dissolved in acetone and then mixed with PEO to obtain a homogeneous solution. The HDI solution was dissolved in a separated beaker and added as cited above to form DCF-loaded polyurea samples. The resulting mixture was poured into Teflon® mold and gelled using the same conditions (temperature and time) than for the pure polyurea. The final materials were named PolyU (polyurea xerogel), PolyU-$DCF_x$ (loaded polyurea containing diclofenac DCF

and *x* for the wt% of drug loaded). Regardless of the polyurea sample (loaded and unloaded) the obtained membranes were transparent and flexible. Formulations of the polyurea samples without and containing diclofenac drug percentage from 1 to 30 wt% are presented in **Table S1**.

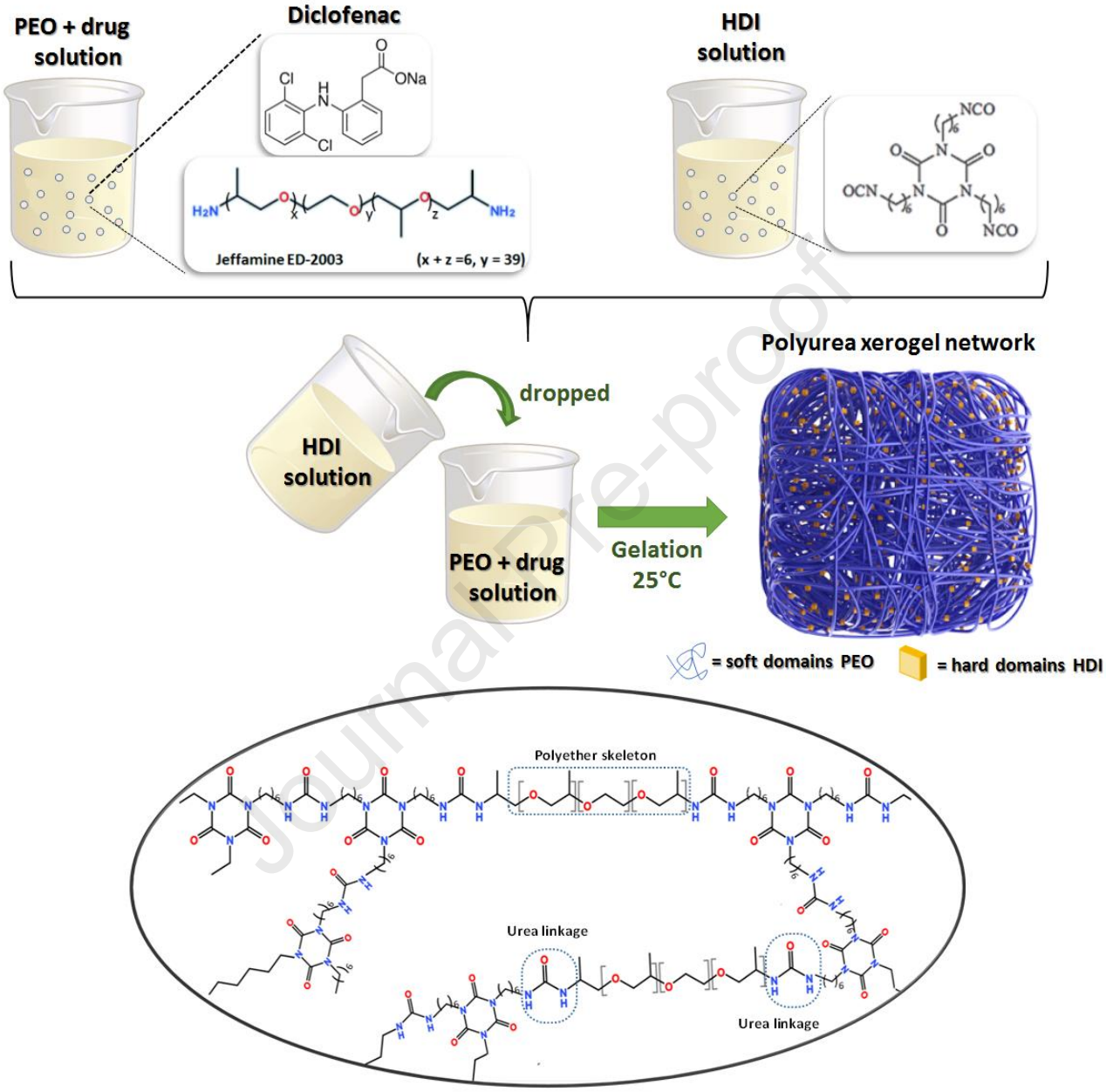


**SCHEME 1**

2.4 *Characterization:*

**Fourier Transform Infrared Spectroscopy** FTIR spectra was recorded at 3100-700 $cm^{-1}$

Journal Pre-proof

by ATR mode using a Perkin Elmer Frontier spectrometer, with a resolution of 4 $cm^{-1}$ and average of 12 scans.

**Small angle X-ray scattering** SAXS experiments were conducted using a Nano-InXider (Xenocs). X-rays of wavelength λ = 1.54 Å was used, and the measurements was performed at sample-to-detector distance of 938 mm to cover a *q*-range of $0.009 < q < 0.45$ $Å^{-1}$, where $q = (4\pi/\lambda) \sin(\theta/2)$ corresponding to the magnitude of the scaterring vector, and $\theta$ is the scaterring angle. Beam size on sample: 400 μm (0.4 mm), typical flux:60 Mph/s, and $Q_{min}$: 0.0044 $Å^{-1}$. All the measurements were recorded at room temperature (~25 °C) using a cell window under vacuum. To collect the SAXS pattern, samples with 1.8 mm ± 0.10 (thickness) and 20 $mm^2$ (area) were used.

**Visual determination of gel time**: In order to evaluate the reactivity (gelation time) of the polyetheramine-PEO and isocyanate HDI, acetone was used as solvent for capping the amines of the polymer chains. In this sense, after the total solubilization of PEO and HDI (separately) the influence of polymer/isocyanate solution contact time with acetone before condensation reaction was studied. The volume of acetone to solubilize PEO and HDI was 7 and 5 mL, respectively. Gelation was considered when the particles present in the initial sol rigidifies the whole wet sol medium. Specifically, condensation reaction was induced by HDI solution added dropwise to the PEO solution. Shortly thereafter, the mixed PEO-HDI solution was spread in an acrylic plate covered by Teflon® using a film extensor. A glass slide was placed on the film without pressure. The gel time was considered when the sol sharply decreased its viscosity converting a viscous liquid state to a gel. The visual experiments were performed on two independent samples, and the results are presented as the data average.

**Differential scanning calorimetry DSC** was used to evaluate the influence of drug content on the glass transition temperature and fusion temperature of crystalline PEO domains. DSC measurements were made using a TA25 DSC. Disk shape of approximately 10 mg were cut off from the polyurea membranes and placed in 40-μL aluminium containers. Each sample was heated from -80 to 250 °C at rate of 10 °C $min^{-1}$ using argon as the purge gas.

**Computational methods**: the geometry optimization of all compounds was performed without constraints and the vibrational frequencies were calculated using the B97D3, [27,28] functional and the 6–31+G(2d,p) basis set (**Table S2**) [29-31]. The 6–31+G(2d,p) basis set provides a good accuracy/efficiency relationship for organic complex systems [32]. Vibrational analyses for all optimized geometries confirm that they are all energy minima at the computational model applied here. Importantly, the molecular electrostatic potential (MEP) [33] surfaces of the: i) isolated drug (diclofenac); and ii) structures derived from polymer polyurea (I–III), were calculated for aid in the choice of the conformations of the complexes investigated (**Figure S1**). These calculations were made using the Gaussian 16 (Revision A.03) software [34]. The bonding mechanism was elucidated through the energy decomposition analysis (EDA) [35] using the BLYP [36,37] functional and Grimmes D3 dispersion correction with Becke–Johnson damping function (D3(BJ)) [38] combined with the TZ2P [39] basis set. These calculations were realized with the ADF2019 package [40].

**Cytotoxicity assay (XTT)**: CHO-K1 cells were cultured in complete medium containing DMEM+HAM F10 (1:1, v/v) (Sigma, St Louis, USA), 10 % fetal calf serum (Sigma, St Louis, USA) and 1% of antibiotics penicillin/streptomycin stabilized solution (Sigma, St Louis, USA) in cell culture flasks of 25 $mm^2$ (TPP, Swizerland). Cells were seeded in 6 (P1), 12 (P2), 24 (P3) or 48 (P4) cell plates with cell growth area of 9.5 $cm^2$, 3.8 $cm^2$, 1.9 $cm^2$ and 0.95 $cm^2$, respectively. After 24 h cell cultures were exposed to a polyurea piece (0,04 $cm^2$) during 48 h, when cell viability was assessed using the Cell Proliferation Assay Kit (Roche) according to manufacture instructions. Percentage of viable cells was calculated considering the negative control as 100% viable after three experimental repetitions. Differences between negative control and experimental groups were evaluated using Analysis of Variance followed by Dunnet's test considering 95% of confidence. Cell media and doxorubicine (1 μM) were used as negative control NC and positive control, respectively.

***In vitro* drug release assays**: temporal release of DCF was evaluated in distilled water (100

Journal Pre-proof

mL, pH 6) using ~ 0.3 g of loaded PolyU containing different amounts of DCF drug. The release assays were carried out at a controlled temperature of 37 °C, under constant stirring (100 rpm). *In vitro* studies were performed by UV-Vis spectroscopy, using a Cary60 dual-beam spectrophotometer (Agilent Technologies) connected to an immersion probe (optical path length of 2 mm). Quantitative determination of the cumulative DCF release were performed using a calibration curve constructed using the maximum absorbance values at $\lambda_{max}$= 275 nm of drug solutions at different concentrations. All the *in vitro* citotoxicity and release experiments were performed with three independent samples, and the results are presented as data average.

## 3. Results and Discussion

### *3.1 Visual gel time*

Gel formation from polyureas occurs as the condensation reaction proceeds. Several parameters can affect the rate of this reaction. Indeed, amines are highly reactive in presence of isocyanates, thus acetone was used to capp the amine groups of polyetheramine-PEO and to evaluate the time of the gelation. **Figure 1** shows gelation time of the polyurea samples as a function of contact time of PEO and HDI with acetone before their mixing (i.e. condensation reactions). We observed that the contact time of the solutions (polyetheramine and HDI) with acetone clearly reduces the reactivity of the polyether. Depending on their applications, e.g. coating or spray processes, the combination of acetone solvent with fast gelation time is an important issue to eliminate energy consumming baking ovens or dryers. **Figure 1** highlights the control over gel time formation (from minutes to hours) by using acetone as solvent which decreases the reactivity between amino groups (from polyether) with isocyanate. The contact time chosen for the rest of the study (PolyU as carrier) was 90 min.

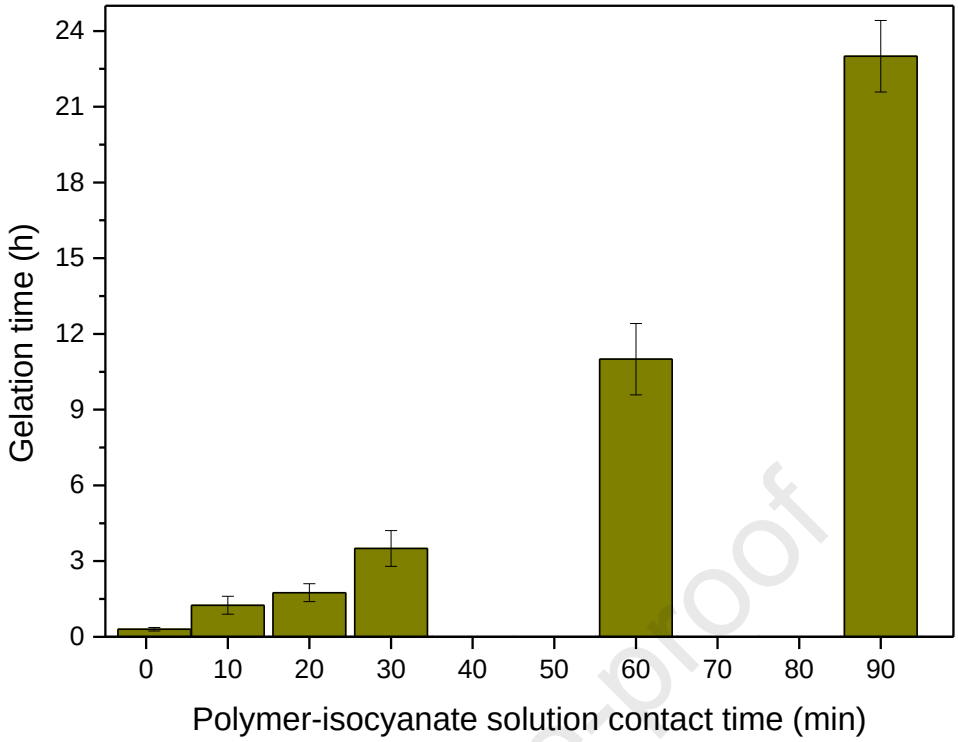


**Figure 1**

*3.2 Structural characterization and theoretical studies*

FTIR studies were performed to evaluate the possible interactions between polyurea matrix and DCF as a function of drug content (1-30 wt%). **Figure 2** shows the FTIR spectra of unloaded and loaded PolyU with the DCF drug from 1750 – 1400 $cm^{-1}$ (**Figure 2a**) and 1300 – 700 $cm^{-1}$ (**Figure 2b**). Regardless of the polyurea matrix (unloaded and loaded), the presence of bands centered at 1636 $cm^{-1}$ (C=O amide I) and 1560 $cm^{-1}$ (CO-N-H amide II) evidences the formation of urea groups (**Figure 2a**). It is important to note the absence of the peak at 2262 $cm^{-1}$ (characteristic of the free isocyanate reactive group from HDI) and the presence of a band at ~3346 $cm^{-1}$ (N-H ν, hydrogen-bond) [25] (**see Figure S2 for full FTIR spectra).** These results indicate the sucessful completion of the reaction between isocyanate and amino groups, after gelation process and curing at room temperature, and thus the formation of the polyurea network.

The polyether region (from 1300 – 700 $cm^{-1}$, **Figure 2b**) shows the characteristic bands at 1142, 1102, 948 and 846 $cm^{-1}$, attributed to the ethylene rocking vibrations ($CH_2$ r) and stretching

Journal Pre-proof

vibrations of the polyether PEO backbone (C–O–C ν) [26]. The FTIR spectrum of PolyU-DCF$_x$ (x = 1-10) closely resembles to the one of PolyU (**Figure 2a,b**): At low concentrations, the vibration bands characteristic of DCF are not observed. As DCF content increases (15 and 30 wt%), bands arise around 1576, 1586 and 1609 cm$^{-1}$, and are attributed to the $O_1C_8O_2$ asymmetric stretching vibration, and the dichlorophenyl and phenylacetate rings streching vibrations, respectively (**Figure 2a**). By comparing the spectrum of PolyU -DCF30 with the spectrum of DCF (ilustrated in **Figure S3a**) one can clearly see a shift of bands centered at 1605, 1589 and 1574 cm$^{-1}$, characteristic of the DCF vibrations cited above. The polyether-PEO characteristic vibration bands do not show changes in both frequency and peak position upon incorporation of the drug at any of the loaded amount (**Figure 2b**). Furthermore, similar emerging and shift of the bands characteristic of DCF drug can be noticed around 718, 749 and 780 cm$^{-1}$ for the loaded polyurea samples with high DCF content (15-30 wt%, see details **Figure 2b**, and **Figure S3b**). These results indicate the existence of polyurea-DCF interactions that will be discussed below.

Journal Pre-proof

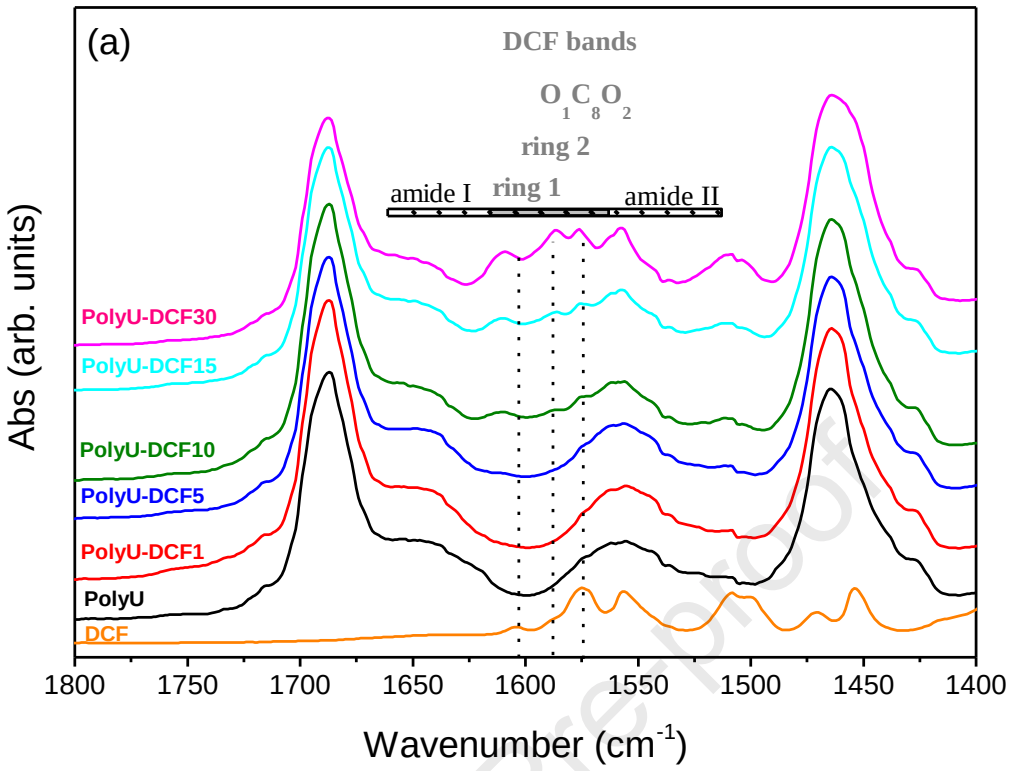


237

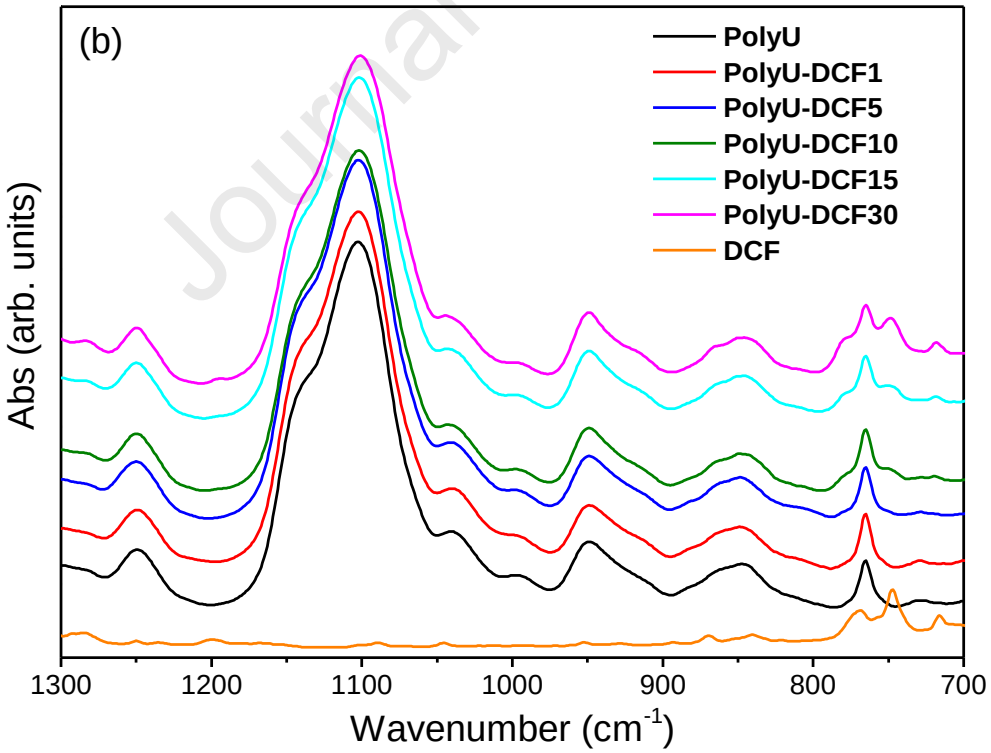


238
239

240 **Figure 2**

241

Journal Pre-proof

To evaluate the interactions between the DCF and the polyurea, we performed computational studies using an energy decomposition analysis (EDA) looking at three representative structures of the polymer network (See compounds **I**–**III** in **Figure S4**). The main results are presented in **Table 1**. According to the EDA formalism [34], the interaction energy, $\Delta E_{int}$, is the summation of several terms corresponding to electrostatic, $\Delta V_{elstat}$, Pauli repulsions, $\Delta E_{Pauli}$, orbital interactions, $\Delta E_{oi}$, and dispersion $\Delta E_{disp}$, components. The term $\Delta V_{elstat}$ represents the quasi–classical electrostatic interaction between unperturbed charge densities and nuclei of the geometrically deformed fragments. The Pauli–repulsion $\Delta E_{Pauli}$ contains the destabilizing interactions between the occupied orbitals and is accountable for the steric repulsion. The orbital interaction $\Delta E_{oi}$ reflects the charge transfer (donor–acceptor interactions between occupied orbitals on one fragment with the empty orbitals of another fragment) and polarization (unoccupied/occupied orbital mixing on one moiety due to the presence of the other). The term $\Delta E_{disp}$ is the dispersion correction contributions [38].

**Figure 3** displays the form of interactions between the selected three polyurea derivates (I-III) and DCF drug. All interactions diclofenac⋯(**I**–**III**) show an attractive nature due to negative values of $\Delta E_{int}$. In addition, these interactions are predominantly electrostatic due to the largest contribution (~ 46%) of $\Delta V_{elstat}$ to the sum of all attractive energetic components $\Delta V_{elstat} + \Delta E_{oi} + \Delta E_{disp}$. However, it is important to highlight that in the DCF⋯(**I** and **II**) complexes, there is also a relevant contribution of the $\Delta E_{oi}$ component (41% and 26%) and a non–negligible role of the $\Delta E_{disp}$ term (12% and 28%). The interactions diclofenac⋯**III** are dispersion dominated, because of the largest contribution of the $\Delta E_{disp}$ energy (43%) to the sum $\Delta V_{elstat} + \Delta E_{oi} + \Delta E_{disp}$. Nevertheless, the diclofenac⋯**III** interactions also show an important contribution of the $\Delta V_{elstat}$ term (34 %) and a non–irrelevant weight of the $\Delta E_{oi}$ component (23 %) to $\Delta V_{elstat} + \Delta E_{oi} + \Delta E_{disp}$. Therefore, the analysis of the interactions diclofenac⋯(**I**–**III**) shows that the drug can establish favorable interactions with the polymer in different bond sites. Furthermore, *in silico* studies suggest that the

268 major binding mechanisms involved hydrogen bonds, in particular between hydrogen atoms from
269 urea groups and diclofenac oxygen atoms.
270

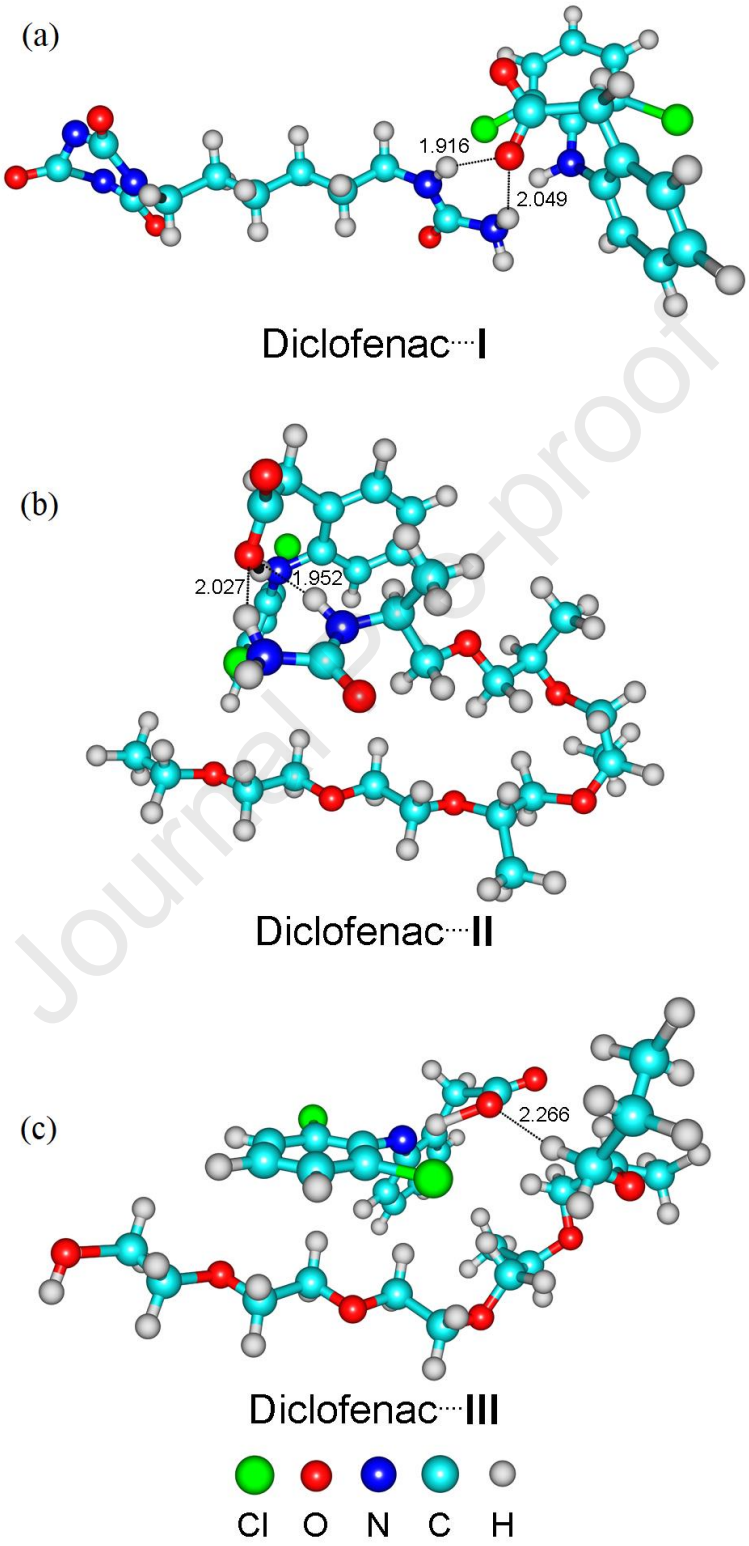


271

272 **Figure 3**

273

Journal Pre-proof

SAXS experiments were conducted to elucidate the microphase separation of the hard domains embedded in the soft domains. **Figure 4** shows the SAXS diffractograms of PolyU and PolyU-DCF30. The presence of a broad peak at q= 1.15 $nm^{-1}$ for PolyU (black circles) is characteristic of the average distance ($\xi$ = 54.6 Å, calculated from $\xi = 2\pi/q_{max}$ ) between the hard and soft domains [25,26]. The connection between triisocyanates groups (from isocyanurate rings of HDI reagent) and polyetheramine-PEO generates microphase separation with distances as show in the inset of **Figure 4**. This broad signal almost dissapears upon incorporation of the drug (**Figure 4, purple squares**) suggesting that the diclofenac molecules are coordinated to different bond sites within the polymer (agreement with computational studies). This feature also strongly indicates that the polyurea favors the high solubility of the drug within the polyether network. These results are in line with thermal properties of polyurea as a function of drug amount loaded discussed below.

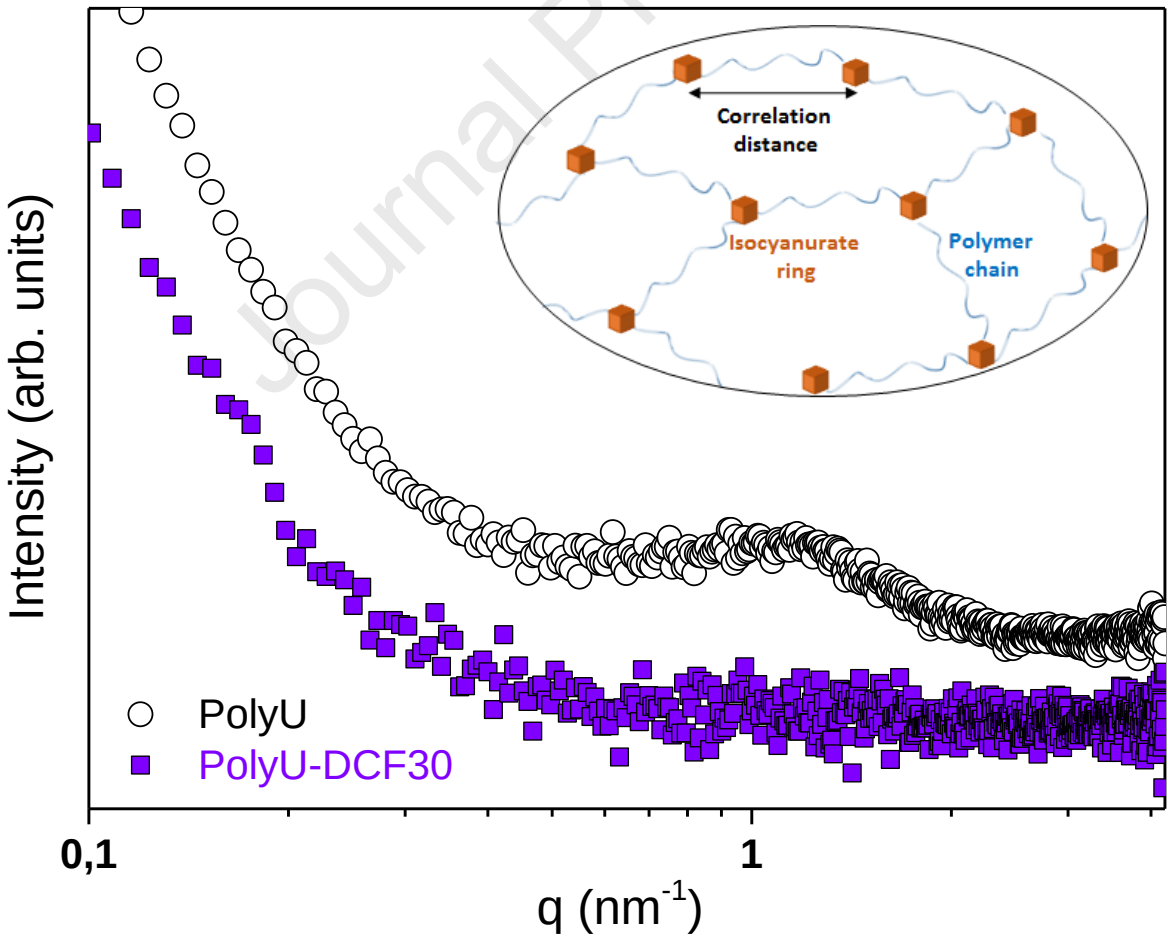


**Figure 4**

Journal Pre-proof

Journal Pre-proof

*3.3 Thermal features*

DSC experiments were conducted for evaluating the influence of DCF drug in both, amorphous phase (glass transition $T_g$) and semi-crystalline moities of the polyurea network. All PolyU xerogels (unloaded and loaded with drug 1 – 30 wt%) showed a unique glass transition ($T_g$) and one melting temperature ($T_m$), **Figure 5a**. These two events ($T_g$ and $T_m$) in DSC thermograms are characteristic of the polyether-PEO chain length and of the ethylene oxide moities crystallization, respectively [41,42]. For PolyU (**Figure 5a black line),** $T_g$ and $T_m$ events were observed at approximately -58 °C and 21 °C, respectively. The great miscibility (solvation) of DCF within PolyU was confirmed by the existence of an unique $T_g$ and the dependency of $T_g$ values with the DCF content (**Figure 5a**). **Table 2** presents the glass transition and melting temperatures as well as the degree of crystallization ($D_c$) deduced from the DSC thermograms. The $T_g$ was characterized by step changes in the heat capacity, and $T_m$ can be obtained from the onset of the endothermic peak, while the crystallinity degree $D_c$ (eqn (1)) is calculated using the ratio between the melting enthalpy of semi- crystalline PEO in the polyurea sample and the melting enthalpy of 100% crystalline PEO:

$$D_C = \frac{\Delta H_m}{\Delta H°_m} \times 100\% \qquad (1)$$

where $\Delta H_m$ is the melting enthalpy per gram of PEO in the PolyU sample, and $\Delta H°_m$ is the melting enthalpy for 100% crystalline PEO (188.9 J $g^{-1}$) [43].

Upon DCF incorporation (1 – 30 wt%), significant changes are observed in the DSC thermograms and the $T_g$/$T_m$ values (**Figure 5a, Table 2**). The presence of the drug through the polyurea network generates three main effects: (i) a significant increase in the glass transition $T_g$ temperature from -58ºC (PolyU) to -35ºC (PolyU-$DCF_{30}$); (ii) a shift of the melting peak temperature centered at 21°C (PolyU) followed by a decrease of the crystallinity degree $D_c$ and (iii) the appearance of a cold-crystallization characterized by an additional exothermic event between -50°C and 14°C. The linear and significant increase in $T_g$ values (**Figure 5b**) and the decrease in the $D_c$ , followed by a $T_m$ shift (from 21°C to 29°C) as a function of the drug loading (see details in

Journal Pre-proof

**Table 2**) evidence the great solvation of DCF. Due to the presence of functional groups such as urea and ether-type oxygen atoms (from polyether), high drug incorporation capability is achieved by the polyurea network. These results are in good agreement with the theoretical and FTIR studies. Furthermore, by incorporating a large amount of DCF (30 wt%) into PolyU, the coordination of the drug through the semi-crystalline domains of PEO leads to a fully amorphous matrix (absence of exothermic event characteristic of melting temperature of semi-crystalline phase, **Figure 5a, pink line**). In this work, the inhibition of the PEO chains crystallization upon DCF coordination with urea groups and polyether oxygens is an additional proof for the full solvatation of DCF molecules. In addition, the glass transition $T_g$ values and crystallinity degree $D$c (**Figure 5b)** show a linear evolution with the increase of the DCF content, traducing an increase of the rigidity and a decrease of the semi-crystalline domains amount, respectively. The inhibition of crystallization of the PEO chains as a function of drug content is illustrated in **Figure 5c**. No crystallization of the PEO is observed when a high amount of DCF drug is incorporated (**Figure 5a pink line and Figure 5c illustration of PEO amorphous structure**), indicating a very rigid polyurea network with reduced chain mobility (see $T_g$ values in **Table 2**).

Journal Pre-proof

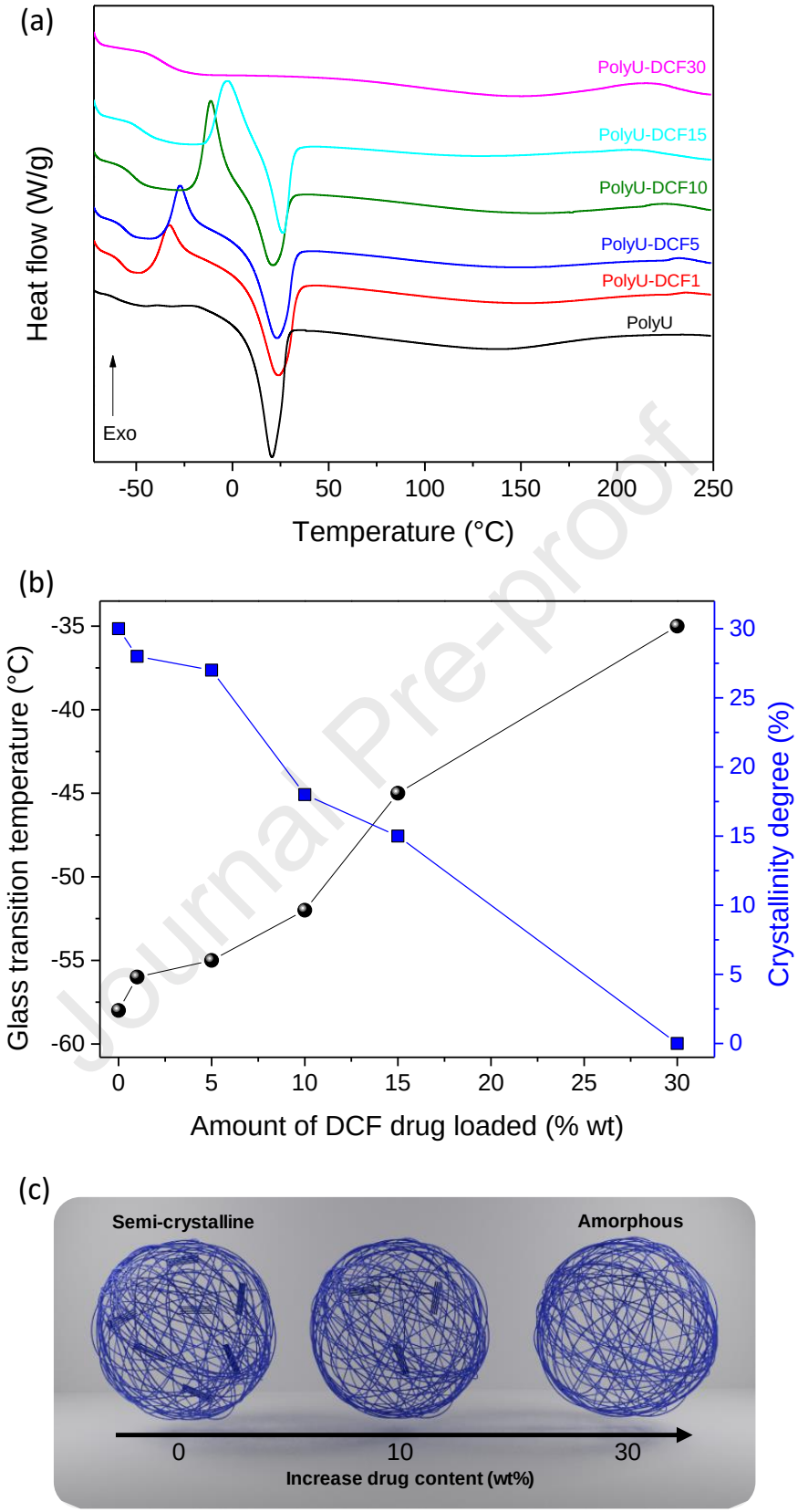
(a)
Heat flow (W/g)
PolyU-DCF30
PolyU-DCF15
PolyU-DCF10
PolyU-DCF5
PolyU-DCF1
PolyU
Exo
-50
0
50
100
150
200
250
Temperature (°C)
(b)
Glass transition temperature (°C)
-35
-40
-45
-50
-55
-60
Crystallinity degree (%)
30
25
20
15
10
5
0
0
5
10
15
20
25
30
Amount of DCF drug loaded (% wt)
(c)
Semi-crystalline
Amorphous
0
10
30
Increase drug content (wt%)

**Figure 5**

*3.4 Citotoxicity evaluation*

The evaluation of medical devices follows the International Organization for Standardization (ISO) rules that recommend : "*in vitro* test methods, which are appropriately validated, reasonably and practically available, reliable and reproducible shall be considered for use in preference to *in vivo* tests" [44]. The polyurea sample was exposure to cells by direct contact with culture medium according to ISO (2003) [45]. Thus, it mimics the physiological conditions by a zone of diffusion in which could affects cellular trauma in accordance with the density of materials [46,47]. According to **Figure 6**, no statistical differences were observed in terms of citotoxicity between cells exposed to PolyU membrane and the negative control (P>0.05). The use of cell plates with different cell growth area did not interfere in cell response to the presence of PEO. Moreover, the CHO-K1 cells are recommended by the Organization for Economic Co-operation and Development (OECD, 2016) for guideline applied to genotoxicity testing of chemicals.

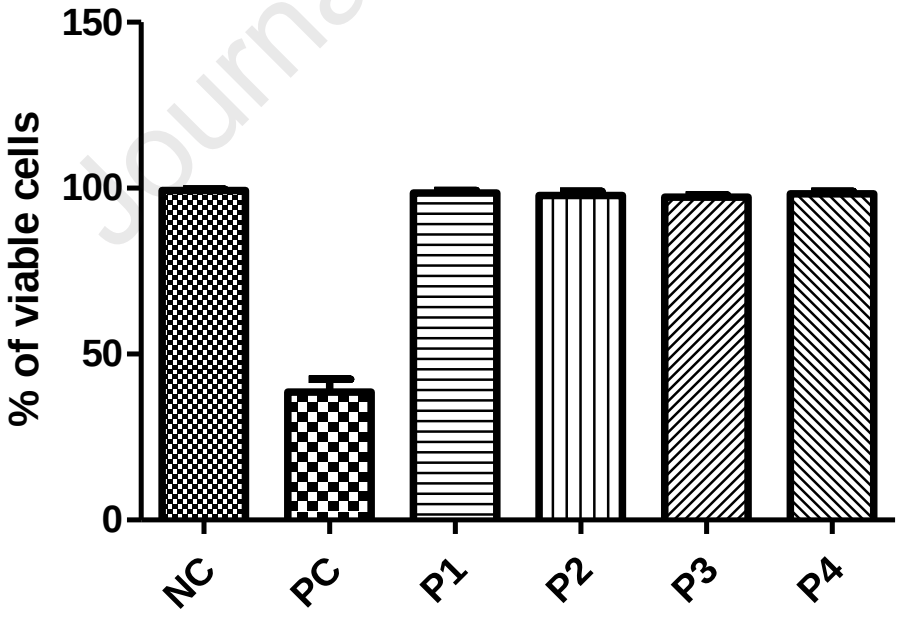


**Figure 6**

Journal Pre-proof

Journal Pre-proof

*3.5 In vitro diclofenac release assays*

The cumulative release of DCF incorporated into polyurea xerogel as a function of drug loading (1 – 30 wt%) are shown in **Figure 7**. The release rate of DCF is low for polyurea samples containing 1 and 5 wt% of DCF, with only a 13 and 36% release after 1440 min, respectively (**Figure 7 red and blue squares**). For the polyurea matrices loaded with 10 – 30 wt% of DCF (**Figure 7 green, cyan and purple squares**), the release rate was higher compared to samples with lower amounts of drug incorporated (1 – 5 wt%).

The release rate of DCF may be described by simultaneous swelling front (water uptake) and DCF release. To explain such a facile solvation (solubilization) of the drug through the polymer backbone, we hypothesized interactions between PEO chains and diclofenac DCF. By increasing the DCF amount loaded in polyurea xerogel a consequent augmentation of drug molecules present on the surface (physisorbed) leads to a high cumulative release of the DCF until ~80% (**Figure 7 purple squares**). These results are in line with FTIR, theoretical, SAXS and DSC studies which demonstrate i) interactions between DCF and the host matrix with the shift of the drug characteristic bands in the FTIR spectrum, ii) favorable interactions with the polymer depending on the bonding site, iii) evident decrease of the peak intensity in the SAXS pattern of the host and iv) clear changes in glass transition temperature ($T_g$) followed by the inhibition of the polymer-PEO crystalline moities as a function of drug load. Here, the tuning of the cumulative release profiles (low or high DCF amount released) have proven valuable in drug delivery applications, due to the ability to easily encapsulate DCF molecules into polyurea by direct dissolving the drug in the PEO polymer. Thus, this class of polyurea xerogel points out the precise control of DCF release by adjusting the amount of drug loaded into polymer matrix.

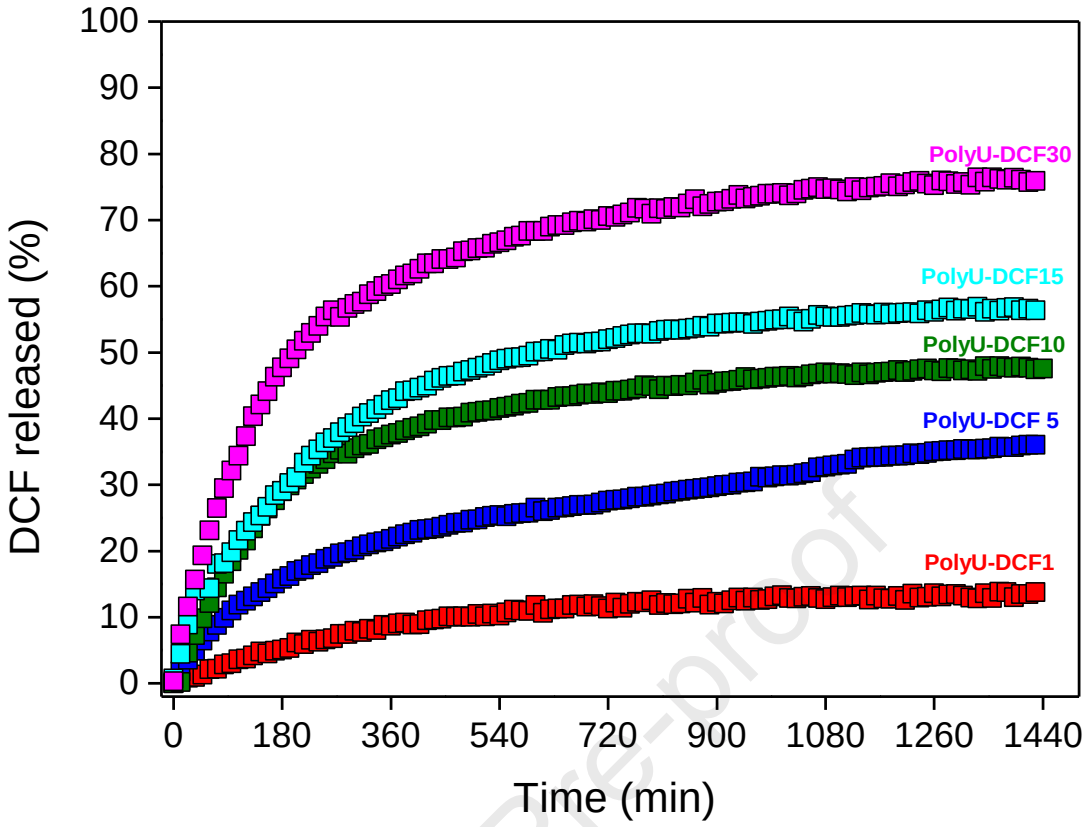


**Figure 7**

The release mechanism of the diclofenac from the loaded PolyU xerogel (1 – 30 wt%) was evaluated by Korsmeyer-Peppas equation [48] (eq. 2), where $M_t$ is the solute mass released at time t, $M_\infty$ is the initial solute mass, $M_t/M_\infty$ is a fraction of the drug released at time *t*, *k* is the released rate constant and *n* is the released exponent which gives information regarding the drug transport mechanism [48]. Depending on the *n* value, different mehanisms can be envisioned: a Fickian diffusion (*n* value of ≤ 0.50), a case II transport indicated by a zero-order drug release (*n* value of ≥ 1), while an anomalous non-Fickian transport mechanism (swelling as well diffusion) is indicated by a *n* value of 0.50 < n < 1.0.

$$\frac{M_t}{M_\infty} = k\, t^n \qquad (2)$$

**Figure 8** shows the release curves, plotted as log ($M_t/M_\infty$) *vs*. log *t*, for loaded PolyU

Journal Pre-proof

containing from 1 – 30 wt% of diclofenac. The kinetic curves of DCF loaded PolyU ( 1 – 30 wt %) samples were well fitted with the Korsmeyer-Peppas model (one straight line - **Figure 8a,b**) showing a coefficient of determination ($R^2$) for all samples of about 0.99. For the PolyU samples containing between 5 and 30 wt% of diclofenac drug the experimental *n* values (see details in **Table S3**) indicate an anomalous transport followed by diffusion/zero-order rate of drug controlled by the penetration of the water-swollen front. For PolyU-$DCF_1$, the calculated *n* value being close to 1, it suggests a Case II transport mechanism for which DCF drug release is mainly controlled by the swelling effect of the polyurea matrix. The cumulative drug released by PolyU-$DCF_1$ sample, suggests that the amount of DCF molecules available near the monolithic surface is low and that entrapped DCF molecules begin to release by water uptake, at slow rate due to the DCF-PEO chains interactions.

Recently, we demonstrated the possibility to incorporate simultaneously an anti-inflamatory and an anticancer drug into a polyurea xerogel for dual delivery purposes [23]. A low loading of amount of drugs (1 wt%) was used to evaluate the potential applications of polyurea as drug delivery system. Herein, we highlight a facile and reproducible control over the amount of drug encapsulated into polyurea xerogel in which 30 wt% of drug load can be easily reached and its release profile can be modulated by the interactions with the host matrix. Moreover, the influence of the drug amount loaded into structural/thermal polyurea properties was in depth correlated.

A cost estimation to produce polyurea PolyU using the synthesis conditions of this work was evaluated. By using the identifiable components values at the laboratory scale prices to obtain three polyurea membranes, the estimated cost (the summation of individual cost elements) was approximately US$ 2.00 (see **Table S4** and **Figure S5**). Due to their physico-chemical properties, biocompatibility, easy-shaping, high capacity of drug loading, and low-cost production these polyurea materials could be fabricated as contact lenses, films, microcapsules, bulky materials and more, with broad implications for many fields. This work has clearly opened up highly interesting prospects for the polyurea as biomaterials. Several aspects derived from the results reported here

412 need to be investigated in the future, such as *in vivo* assays.

413

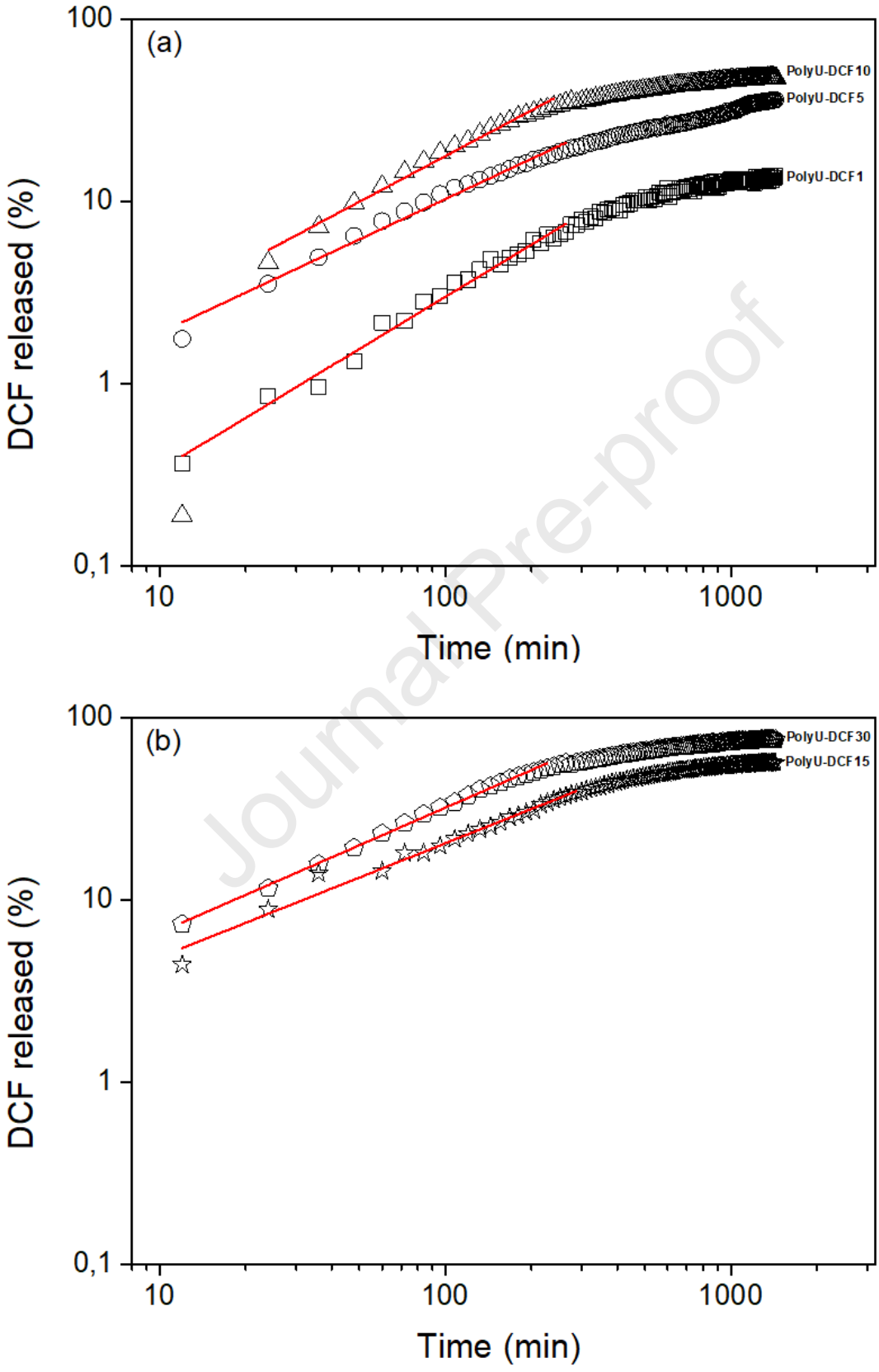


414

415 **Figure 8**

Journal Pre-proof

## 4. Conclusions

A polyurea xerogel (PolyU) was synthesized by reaction between a polyetheramine (PEO) and an aliphatic poliisocyanate (HDI). The PolyU matrix shows a high encapsulation capability of a model drug diclofenac sodium (DCF) up to 30 wt%. Due to the sol-gel process, the simplicity of industrial scale-up in the gel preparation at room temperature is also an important point favoring their development as potential drug delivery vehicle. PolyU gel time formation could be controlled (from mintutes to hours) by the solvent contact time of the PEO and HDI before the condensation reactions (mixture) between both reagents. We demonstrated novel insights into biological and physical chemical properties of this class of polyurea xerogel containing DCF. In this sense, the characterization of the materials shows a good correlation between the techniques used such as FTIR, SAXS and DSC analysis. The existence of PolyU-DCF interactions (hydrogen bonds) was confirmed by i) experimental FTIR/theoretical in silico results; ii) by SAXS with the dissapearance upon high DCF loading of the broad signal evidencing microphase separation and spacial correlation between hard domains embedded in the polymeric matrix; iii) by thermal features highlighting that the fraction of the crystalline polymer-PEO (endothermic fusion peaks in DSC thermograms) was drastically affected as a function of DCF loading, indicating a stable compatible mixture of the pair polyurea-drug leading to a complete amorphous polymeric nature and iv) by the exposure of PolyU xerogel to CHO-K1 cells which shows a high cell viability suggesting that polyurea matrix could be used as biomaterials. A precise control over DCF relase was demonstrated by the judicious choice of the drug loading amount into the PolyU matrix. The use of this class of polyurea containing drugs open positive perspectives finding applications from drug delivery systems like transdermal delivery patches, encapsulation for food formulation, beverages and cosmectics.

**Conflicts of interest**: There are no conflicts to declare.

**Acknowledgements:** The authors would like to thank Celso V. Santilli and Rodrigo Santos for small angle X ray scattering measurements (SAXS -EMU Instituto de Química - Câmpus de Araraquara), thank

Journal Pre-proof

Huntsman Performance Products and Bayer Group for donating the Jeffamine® and triisocyanate crosslinker reagents, respectively. The authors are grateful to funding agencies CAPES (Finance Code 001), CNPq (307696/2021-9), and FAPESP grant (n° 2021/06552-1 and SPRINT 2017/50286-9) and CNRS (PRC Clustobrane).

## References

[1] D. Moorkoth, K. M. Nampoothiri, S. Nagarajan, A. R. Girija, S. Balasubramaniyan, D. S. Kumar, Star-Shaped Polylactide Dipyridamole Conjugated to 5-Fluorouracil and 4-Piperidinopiperidine Nanocarriers for Bioimaging and Dual Drug Delivery in Cancer Cells, *ACS Appl. Polym. Mater.* 3 (2021), 737-756.

[2] Y. Guo, Y. Li, S. Zhou, Q. Ye, X. Zan, Y. He, Y. Charged Poly(N-isopropylacrylamide) Nanogels for the Stabilization of High Isoelectric Point Proteins, *ACS Biomater. Sci. Eng.* 7 (2021), 4282–4292.

[3] L. Xu, H. Wang, Z. Chu, L. Cai, H. Shi, C. Zhu, D. Pan, J. Pan, X. Fei, Y. Lei, Temperature-Responsive Multilayer Films of Micelle-Based Composites for Controlled Release of a Third-Generation EGFR Inhibitor, *ACS Appl. Polym. Mater.* 2 (2020), 741–750.

[4] H. Karimi-Maleh, S. J. Mousavi, M. Mahdavian, M. Khaleghi, S. Bordbar, M. L. Yola, R. Darabi, M. Liu, Effects of silver nanoparticles added into polyurea coating on sulfate-reducing bacteria activity and electrochemical properties; an environmental nano-biotechnology investigation, *Environmental Research,* 198 (2021), 111251.

[5] K. Chang, Y. Liu, D. Hu, Q. Qi, D. Gao, Y. Wang, D. Li, X. Zhang, H. Zheng, Z. Sheng, Z. Yuan, Highly Stable Conjugated Polymer Dots as Multifunctional Agents for Photoacoustic Imaging-Guided Photothermal Therapy, *ACS Appl. Mater. Interfaces* 10 (2018), 7012–7021.

[6] D. Babikova, R. Kalinova, D. Momekova, I. Ugrinova, G. Momekov, I. Dimitrov, Multifunctional Polymer Nanocarrier for Efficient Targeted Cellular and Subcellular Anticancer Drug Delivery, *ACS Biomater. Sci. Eng.* 5 (2019), 2271–2283.

[7] M. Hamilton, S. Harrington, P. Dhar, L. Stehno-Bittel, Hyaluronic Acid Hydrogel Microspheres for Slow Release Stem Cell Delivery, *ACS Biomater. Sci. Eng.* 7 (2021), 3754–3763.

[8] C. Cleeton, A. Keirouz, X. Chen, N. Radacsi, Electrospun Nanofibers for Drug Delivery and Biosensing , *ACS Biomater. Sci. Eng.* 5, (2019), 4183–4205.

[9] W. Wang, M. Zhang, L. Chu, Functional Polymeric Microparticles Engineered from Controllable Microfluidic Emulsions, *Acc. Chem. Res.* 47 (2014), 373–384.

[10] M. H. Jandaghian, H. Kazerooni, Performance of polyurea formulations against impact loads: A molecular dynamics and mechanical simulation approach, *J. Appl. Polym. Sci.* 138 (2021), 50309.

[11] M. Soccio, R. Mazzoni, C. Lucarelli, S. Quattrosoldi, A. Cingolani, M. Fiorini, N. Lotti, T. Tabanelli, Urea and Polyurea Production: An Innovative Solvent- and Catalyst-Free Approach through Catechol Carbonate, *ACS Sustainable Chem. Eng.* 8 (2020), 15640-15650.

[12] Y. Zhang, Y. Wan, Y. Li, G. Pan, H. Yu, W. Du, H. Shi, C. Wu, Y. Liu, Thin-film composite nanofiltration membrane based on polyurea for extreme pH condition, *J. Membr. Sci.* 635 (2021), 119472.

[13] N. Reed, N. U. Huynh, Rosenow, B.; Manlulu, K.; Youssef, G. Synthesis and characterization of elastomeric polyurea foam, *J. Appl. Polym. Sci.* 137 (2020), 48839.

[14] D. Zhang, B. Li, X. Zhang, Z. Zhang, W. Wang, F. Liu, Phoxim Microcapsules Prepared with Polyurea and Urea–Formaldehyde Resins Differ in Photostability and Insecticidal Activity, *J. Agric. Food Chem.* 64 (2016), 2841–2846.

[15] G. Holden, N. R. Legge, R. Quirk, H. E. Schroeder, Thermoplastic Elastomers, 2nd ed.; Eds.; Hanser/Gardner Publications: Cincinnati, OH, **1996**.

[16] A. Feula, A. Pethybridge, I. Giannakopoulos, X. Tang, A. Chippindale, C. R. Siviour, C. P. Buckley, I. W. Hamley, W. A. Hayes, Thermoreversible Supramolecular Polyurethane with Excellent Healing Ability at 45 °C, *Macromol.* 48 (2015), 6132–6141.

[17] R. E. Kieltyka, A. C. H. Pape, L. Albertazzi, Y. Nakano, M. M. C. Bastings, I. K. Voets, P. Y. W. Dankers, E. W. Meijer, Mesoscale Modulation of Supramolecular Ureidopyrimidinone-Based Poly(ethylene glycol) Transient Networks in Water, *J. Am. Chem. Soc.* 135 (2013), 11159−11164.

[18] E. Wisse, A. J. H. Spiering, P. Y. W. Dankers, B. Mezari, P. C. M. M. Magusin, E. W. Meijer, Multicomponent Supramolecular Thermoplastic Elastomer with Peptide-Modified Nanofibers, *J. Polym. Sci. A: Polym. Chem.* 49 (2011), 1764–1771.

[19] P. Paraskevopoulou, I. Smirnova, T. Athamneh, M. Papastergiou, D. Chriti, G. Mali, T. Cendak, G. Raptopoulosa, P. Gurikov, Polyurea-crosslinked biopolymer aerogel beads, *RSC Adv.* 10 (2020), 40843–40852.

[20] J. V. John, E. J. Seo, R. Augustine, I. H. Jang, D. K. Kim, Y. W. Kwon, J. H. Kim, I. Kim, Phospholipid End-Capped Bioreducible Polyurea Micelles as a Potential Platform for Intracellular Drug Delivery of Doxorubicin in Tumor Cells, *ACS Biomater. Sci. Eng.* 2 (2016), 1883–1893.

[21] C. Cuscó, J. Garcia, E. Nicolás, P. Rocas, J. Rocas, Multisensitive drug-loaded polyurethane/polyurea nanocapsules with pH-synchronized shell cationization and redox-triggered release, *Polym. Chem.*, 7 (2016), 6457-6466.

[22] K. R. Gajbhiye, B. P. Chaudhari, V. B. Pokharkar, A. Pawar, V. Gajbhiye, Stimuli-responsive biodegradable polyurethane nano-constructs as a potential triggered drug delivery vehicle for cancer therapy, *Int. J. Pharm.* 588 (2020), 119781.

[23] M. A. de Resende, G. A. Pedroza, L. H. G. M. C. Macêdo, R. de Oliveira, R.; M. Amela-Cortes, Y. Molard, E. F. Molina, Design of polyurea networks containing anticancer and anti-inflammatory drugs for dual drug delivery purposes. *J. Applied polymer Sci* 139, (2022), 51970.

[24] A. Sánchez-Ferrer, D. Rogez, P. Martinoty, Synthesis and Characterization of New Polyurea Elastomers by Sol/Gel Chemistry, *Macromol. Chem. Phys.* 211 (2010), 1712–1721.

[25] A. Sánchez-Ferrer, V. Soprunyuk, M. Engelhardt, R. Stehle, H. A. Gilg, W. Schranz, K. Richter, Polyurea Networks from Moisture-Cure, Reaction-Setting, Aliphatic Polyisocyanates with Tunable Mechanical and Thermal Properties, *ACS Appl. Polym. Mater*. 3 (2021), 4070−4078.

[26] N. A. M. de Jesus, R. de Oliveira, M. Amela-Cortes, N. Dumait, S. Cordier, Y. Molard, E. F. Molina, Facile and scalable design of light-emitting and ROS-generating hybrid materials made of polyurea gels embedding a molybdenum cluster-based salt, *Dalton Trans.* 50 (2021), 8907–8916.

[27] A. D. Becke, Density-Functional Thermochemistry. V. Systematic Optimization of Exchange-Correlation Functionals, *J. Chem. Phys.* 107 (1997), 8554–8560.

[28] S. Grimme, S. Ehrlich, L. Goerigk, Effect of the damping function in dispersion corrected density functional theory, *J. Comp. Chem.* 32 (2011), 1456–1465.

[29] P. C. Hariharan, J. A. Pople, The influence of polarization functions on molecular orbital hydrogenation energies, *Theoret. Chimica Acta* 28 (1973), 213–222.

[30] M. M. Francl, W. J. Petro, W. J. Hehre, J. S. Binkley, M. S. Gordon, D. J. de Frees, J. A. Pople, Self-Consistent Molecular Orbital Methods. XXIII. A Polarization- Type Basis Set for Second-Row Elements, *J. Chem. Phys.* 77 (1982), 3654–3665.

[31] M. J. Frisch, J. A. Pople, J. S. Binkley, Self-consistent molecular orbital methods 25. Supplementary functions for Gaussian basis sets, *J. Chem. Phys.* 80 (1984), 3265–3269.

[32] E. F. Molina, R. L. T. Parreira, E. H. de Faria, H. W. P. de Carvalho, G. F. Caramori, D. F. Coimbra, E. J. Nassar, K. J. Ciuffi, Ureasil-Poly(ethylene oxide) Hybrid Matrix for Selective Adsorption and Separation of Dyes from Water, *Langmuir* 30 (2014), 3857−3868.

[33] K. A. Ford, Role of Electrostatic Potential in the in Silico Prediction of Molecular Bioactivation and Mutagenesis, *Mol. Pharm.* 10 (2013), 1171–1182.

[34] Gaussian 16, Revision A.03, M. J. Frisch, G. W. Trucks, H. B. Schlegel, G. E. Scuseria, M. A. Robb, J. R. Cheeseman, G.,Scalmani, V. Barone, G. A. Petersson, H. Nakatsuji, X. Li, M. Caricato, A. V. Marenich, J. Bloino, B. J. Janesko, R. Gomperts, B. Mennucci, H. P. Hratchian, J. V. Ortiz, A. F. Izmaylov, J. L. Sonnenberg, D. Williams–Young, F. Ding, F. Lipparini, F. Egidi, J. Goings, B. Peng, A. Petrone, T. Henderson, D. Ranasinghe, V. G. Zakrzewski, J. Gao, N. Rega, G. Zheng,

Journal Pre-proof

W. Liang, M. Hada, M. Ehara, K. Toyota, R. Fukuda, J. Hasegawa, M. Ishida, T. Nakajima, Y. Honda, O. Kitao, H. Nakai, T. Vreven, K. Throssell, J. A. Montgomery, J. E. Peralta, F. Ogliaro, M. J. Bearpark, J. J. Heyd, E. N. Brothers, K. N. Kudin, V. N. Staroverov, T. A. Keith, R. Kobayashi, J. Normand, K. Raghavachari, A. P. Rendell, J. C. Burant, S. S. Iyengar, J. Tomasi, M. Cossi, J. M. Millam, M. Klene, C. Adamo, R. Cammi, J. W. Ochterski, R. L. Martin, K. Morokuma, O. Farkas, J. B. Foresman, D. J. Fox, Gaussian, Inc., Wallingford CT, **2016**.

[35] F. M. Bickelhaupt, E. J. Baerends, Kohn-Sham Density Functional Theory: Predicting and Understanding Chemistry, *Rev. Comput. Chem.* 15 (2000), 1–86.

[36] A. D. Becke, Density-functional exchange-energy approximation with correct asymptotic behavior, *Phys. Rev. A* 38 (1988), 3098–3100.

[37] C. Lee, W. Yang, R. G. Parr, Development of the Colle-Salvetti correlation-energy formula into a functional of the electron density, *Phys. Rev. B* 37 (1988), 785–789.

[38] S. Grimme, J. Antony, S. Ehrlich, H. Krieg, A consistent and accurate ab initio parametrization of density functional dispersion correction (DFT-D) for the 94 elements H-Pu, *J. Chem. Phys.* 132 (2010), 154104.

[38] E. van Lenthe, E. J. Baerends, Optimized Slater-type basis sets for the elements 1–118, *J. Comput. Chem.* 24 (2003), 1142–1156.

[39] C. F. Guerra, J. G. Snijders, G. T. Velde, E. J. Baerends, Towards an order-N DFT method, *Theor. Chem. Acc.* 99 (1998), 391–403.

[40] E. F. Molina, S. H. Pulcinelli, V. Briois, C. V. Santilli, Fine-tuning of a nanostructure, swelling, and drug delivery profile by blending ureasil–PEO and ureasil–PPO hybrids, *Polym. Chem.* 5 (2014), 1897–1904.

[41] E. F. Molina, C. R. N. Jesus, L. A. Chiavacci, S. H. Pulcinelli, V. Briois, C. V. Santilli, Ureasil–polyether hybrid blend with tuneable hydrophilic/hydrophobic features based on U-PEO1900 and U-PPO400 mixtures, *J. Sol-Gel Sci. Technol.* 70 (2014), 317–328

[43] K. Y. Mya, K. P. Pramoda, C. B. He, Crystallization behavior of star-shaped poly(ethylene oxide) with cubic silsesquioxane (CSSQ) core, *Polymer* 47, (2006), 5035−5043.

[44] ISO 10993-1 (2009). Biological evaluation of medical devices – Part 1: Evaluation and testing within a risk management process. International Organization for Standardization, Geneva, Switzerland.

[45] ISO 10993-1:2003. Biological evaluation of medical devices. Part 1: Evaluation and testing, vol. 10993-1:2003.

[46] H. S. Baek, J. Y. Yoo, D. K. Rah, D. Han, D. H. Lee, O. Kwon, J. Park, Evaluation of the extraction method for the cytotoxic testeing of latex gloves, *Y. Med. J.* 46 (2005), 579-583.

Journal Pre-proof

[47] B. D. Ratner, S. J. Northup, Testing biomaterials, in: Ratner, B.D., Hoffman, A.S., Schoen, F.J., Lemons, J.E. (Eds), Biomaterials science: an introduction to materials in medicine, Academic Press, New York, **1996** pp. 215-220.

[48] R. Korsmeyer, R. Gurny, E. Doelker, P. Buri, N. A. Peppas, Mechanisms of Solute Release from Porous Hydrophilic Polymers, *Int. J. Pharm.* 15 (1983), 25−35.

Journal Pre-proof

Journal Pre-proof

587

588 **Figure Legends**

589 **Scheme 1**. Synthetic route for the preparation of polyurea matrix and schematic network showing
590 hard domains isocyanurate ring (yellow squares) and soft domains polyether chains (blue lines).

591

592 **Figure 1**. Gelation time formation of polyurea networks as a function of monomers contact time
593 with acetone solvent.

594

595 **Figure 2**. FTIR spectra of the unloaded and loaded polyurea PolyU containing different amount of
596 drug (1-30 wt%) in the region between (a) 1750 – 1400 $cm^{-1}$, and (b) 1300 - 7000 $cm^{-1}$.

597

598 **Figure 3:** Equilibrium geometries for the Diclofenac....(I−III) complexes [B97D3/6–31+G(2d,p)].
599 Distances are given in angstroms.

600

601 **Figure 4.** SAXS patterns of the unloaded PolyU and PolyU containing 30 wt% of drug DCF. Inset:
602 schematic representation of the microphases formed between the hard domains and soft domains in
603 the polyurea network and correlation distance between these domais.

604

605 **Figure 5**. (a) DSC thermograms of the unloaded and loaded PolyU containing different amount of
606 drug (1-30 wt%), (b) comparison of both $T_g$ and $T_m$ as a function of drug content, and (c) schematic
607 representation of the semi-crystalline PEO chains with decrease of crystallization degree induced by
608 the increase of diclofenac drug content.

609

610 **Figure 6.** Percentage of CHO-K1 viable cells obtained by XTT assay after 48 h exposure to PolyU
611 membrane (0.04 $cm^2$). The P1-P4 represents different well plates. NC: negative control (cell
612 media); PC: positive control (doxorubicin 1 µM).

613

614 **Figure 7.** Temporal evolution of cumulative amount released for polyurea PolyU containing
615 different amounts of diclofenac drug (1 – 30 wt%)

616

617 **Figure 8.** Plots of log ($M_t/M_\infty$) vs log $t$ for release experiments of PolyU containing different
618 amounts of diclofenac drug (a) 1, 5 and 10 wt%; (b) 15 and 30 wt%.

619

620

621

Journal Pre-proof

622

623 TABLE

624

625 **Table 1.** Analysis of the bonding situation between the DCF drug and structures derived from
626 polymer polyurea (**I**–**III**) through of the EDA method. The energy unit is kcal $mol^{-1}$.[a,b]

627

| Complex | $\Delta E_{int}$ | $\Delta V_{elstat}$ | $\Delta E_{Pauli}$ | $\Delta E_{oi}$ | $\Delta E_{disp}$ |
|---|---|---|---|---|---|
| Diclofenac····**I** | –53.40 | –39.92 (47) | 30.88 | –34.23 (41) | –10.12 (12) |
| Diclofenac····**II** | –36.70 | –34.01 (46) | 37.05 | –19.05 (26) | –20.70 (28) |
| Diclofenac····**III** | –27.61 | –19.64 (34) | 29.97 | –13.10 (23) | –24.83 (43) |

628 [a] $\Delta E_{int} = \Delta V_{elstat} + \Delta E_{Pauli} + \Delta E_{oi} + \Delta E_{disp}$; [b] Values in parentheses correspond to the percentage of each stabilizing contribution
629 ($\Delta V_{elstat} + \Delta E_{oi} + \Delta E_{disp} = 100\%$).

630

631

632

633

634

635 **Table 2.** Thermal characteristics determined by DSC measurements of the unloaded and loaded Pug
636 containing different amount of DCF drug from 1 to 30 wt%.

637

| ***Sample*** | $T_g$ **(°C)** | $T_m$ ***(°C)*** | $D_c$ ***(%)*** |
|---|---|---|---|
| PolyU | -58 | 21 | 30 |
| PolyU-DCF1 | -56 | 23 | 28 |
| PolyU-DCF5 | -55 | 23 | 27 |
| PolyU-DCF10 | -52 | 21 | 18 |
| PolyU-DCF15 | -45 | 29 | 15 |
| PolyU-DCF30 | -35 | - | - |

638

639

640

641
642
643

Journal Pre-proof

Graphical abstract

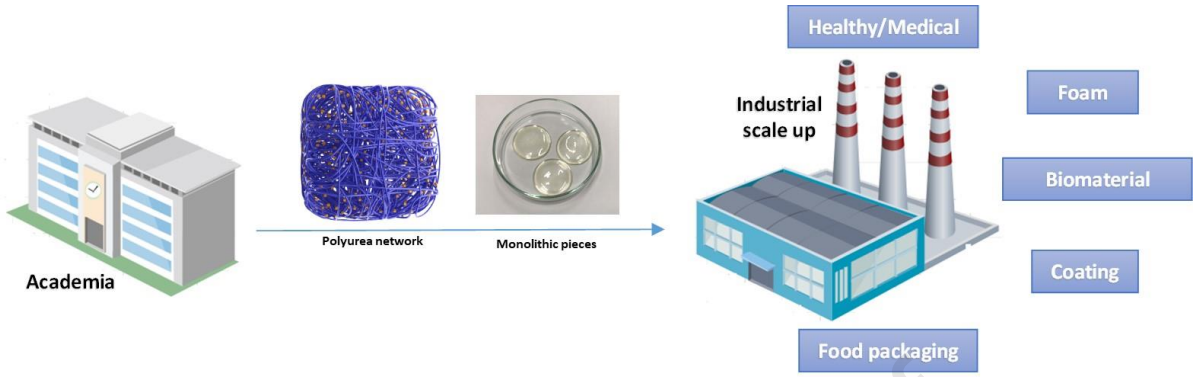


Journal Pre-proof

Journal Pre-proof

Highlights

Facile control over diclofenac drug release Kinects is described

Polyurea provide promising opportunities for scale up fabrication new functional devices

Versatile and cost-efficient carrier for drug delivery application

High amounts of anti-inflammatory drug loaded into polymer matrix

Journal Pre-proof

Journal Pre-proof

# Cost-efficient Polyurea Carrier for Precise Control of an anti-inflammatory Drug Loading and Release

*Gabriele A. Pedroza,[1] Lucia H. G. M. C. Macedo,[1] Ricardo de Oliveira,[1] Natália S. Nascimento,[1] Renato P. Orenha,[1] Renato L. T. Parreira,[1] Raquel Santos,[1] Yann Molard,[2] Maria Amela-Cortes,[2] Eduardo F. Molina*[*1]*

[1]*Universidade de Franca, Av. Dr. Armando Salles Oliveira 201, 14404-600 Franca, SP, Brazil*

[2]*Université Rennes, CNRS, ISCR - UMR 6226, ScanMAT – UMS 2001, F-35000 Rennes, France*

Journal Pre-proof

**Credit author statement**

G. A. Pedroza is the main author contributing in all steps. L. H. G. M. C. Macedo and R. de Oliveira performed gel time formation, drug delivery assays and FTIR measurements. N. S. Nascimento and R. Santos performed the cytotoxicity studies. R. L. T. Parreira and R. P. Orenha work on theoretical studies. Y. Molard and M. Amela-Cortes performed DSC analysis and worked on the results and discussion. E. F. Molina (supervisor of G. A. Pedroza) suggested the experiments, discussed the results and wrote the manuscript. All authors read and commented on the manuscript.

Journal Pre-proof

**Declaration of interests**

☒ The authors declare that they have no known competing financial interests or personal relationships that could have appeared to influence the work reported in this paper.

☐The authors declare the following financial interests/personal relationships which may be considered as potential competing interests:

Journal Pre-proof